

Fe–C and Fe–H systems at pressures of the Earth's inner core

Z G Bazhanova, A R Oganov, O Gianola

DOI: 10.3367/UFNe.0182.201205c.0521

Contents

1. Introduction	489
2. Methodology	491
3. Structures and compositions of stable iron carbides at ultrahigh pressures	492
4. Structures and compositions of stable iron hydrides at ultrahigh pressures	493
5. How much carbon and hydrogen are needed to explain the density of the inner core?	494
6. Conclusions	496
References	496

Abstract. The solid inner core of Earth is predominantly composed of iron alloyed with several percent Ni and some lighter elements, Si, S, O, H, and C being the prime candidates. To establish the chemical composition of the inner core, it is necessary to find the range of compositions that can explain its observed characteristics. Recently, there have been a growing number of papers investigating C and H as possible light elements in the core, but the results were contradictory. Here, using *ab initio* simulations, we study the Fe–C and Fe–H systems at inner core pressures (330–364 GPa). Based on the evolutionary structure prediction algorithm USPEX, we have determined the lowest-enthalpy structures of all possible carbides (FeC, Fe₂C, Fe₃C, Fe₄C, FeC₂, FeC₃, FeC₄, Fe₇C₃) and hydrides (Fe₄H, Fe₃H, Fe₂H, FeH, FeH₂, FeH₃, FeH₄) and have found that Fe₂C (space group *Pnma*) is the most stable iron carbide at pressures of the inner core, while FeH, FeH₃, and FeH₄ are the most stable iron hydrides at these conditions. For Fe₃C, the cementite structure (space group *Pnma*) and the *Cmcm* structure recently found by random sampling are less stable than the *I-4* and *C2/m* structures predicted here. We have found that FeH₃ and FeH₄ adopt chemically interesting thermodynamically stable crystal structures, containing triva-

lent iron in both compounds. We find that the density of the inner core can be matched with a reasonable concentration of carbon, 11–15 mol.% (2.6–3.7 wt.%) at relevant pressures and temperatures, yielding the upper bound to the C content in the inner core. This concentration matches that in CI carbonaceous chondrites and corresponds to the average atomic mass in the range 49.3–51.0, in close agreement with inferences from Birch's law for the inner core. Similarly made estimates for the maximum hydrogen content are unrealistically high: 17–22 mol.% (0.4–0.5 wt.%), which corresponds to the average atomic mass of the core in the range 43.8–46.5. We conclude that carbon is a better candidate light alloying element than hydrogen.

1. Introduction

The problem of determination of the chemical composition of the Earth's core has fascinated geoscientists, physicists, chemists, and materials scientists for several decades. It is clear that iron-based alloys are the dominant components of Earth's solid inner core and liquid outer core, but according to seismic models, the density of the core is several percent lower than the density of pure iron or an iron–nickel alloy at relevant pressures and temperatures [1–3]. From Birch's law [4], one can deduce that the mean atomic mass in the core is ~49 [5], while for pure iron it is 55.85. To explain these differences, one has to allow for ~10–20 mol.% of lighter elements [1–3, 6, 7]. Poirier [8], considering four postulates of Stevenson [2], has specified Si, S, O, H, and C as the likeliest candidates. Initially, relatively few papers considered carbon and hydrogen as major light elements in the core, but recently the number of studies has increased dramatically. There is little consistency among published studies on this issue, and here we want to analyze it avoiding assumptions and extrapolations that have previously led to long-standing controversies.

According to Wood [9], “carbon is extremely abundant in the Solar System (10 × Si, 20 × S), in CI carbonaceous chondrites (3.2 wt.%), and it dissolves readily in liquid Fe at low pressures (4.3 wt.% at 1420 K). Despite these properties it is rarely considered a potential light element in the Fe-rich core, because it is volatile, even at low temperatures, as CO.”

Z G Bazhanova Scientific Research Computer Center, Lomonosov Moscow State University, Leninskie gory 1, str. 4, 119991 Moscow, Russian Federation
Tel. + 7 (495) 939 54 31. Fax + 7 (495) 938 21 36
E-mail: bazhanov@srcc.msu.ru

A R Oganov Department of Geosciences and Department of Physics and Astronomy, Stony Brook University, Stony Brook NY 11794-2100, USA
Tel. + 1 (631) 632 14 29. Fax + 1 (631) 632 82 40
E-mail: artem.oganov@sunysb.edu

Geology Department, Lomonosov Moscow State University, Leninskie gory, 119991 Moscow, Russian Federation

O Gianola Department of Earth Sciences, Institut für Geochemie und Petrologie, ETH Zürich, Clausiusstrasse 25, 8092 Zürich, Switzerland
E-mail: omar.gianola@erdw.ethz.ch

Received 13 December 2011, revised 22 February 2012
Uspekhi Fizicheskikh Nauk **182** (5) 521–530 (2012)
DOI: 10.3367/UFNr.0182.201205c.0521
Translated by authors

Nevertheless, Wood [9] concluded that carbon should be considered as a possible light component of the core, because its volatility decreases and solubility in liquid iron increases with increasing pressure. However, Poirier [8] noted that even at high pressures carbon's solubility in iron remains insufficient to explain the density deficit of the core. Tingle [10] proposed that carbon was incorporated in the core during its formation, and as supporting evidence used the observed large amounts of carbon in iron meteorites, as well as experiments on its high-pressure solubility in liquid iron [9, 11]. Estimates of carbon content in the inner core range from 0.2 wt.% [12] to 4 wt.% [13]. Based on shock-wave and seismic data, Anisichkin [14] advocated carbon as a major light element (as much as 10 wt.%) in the core, and possibly in the diamond phase. However, from first-principles calculations [15, 16] it became clear that diamond cannot be present in the core, because diamond reacts with iron at high pressures, forming iron carbides. Experimental results by Tateno et al. [17], obtained at pressures and temperatures of the Earth's inner core, indicate a low solubility of carbon in iron and the coexistence of iron with some iron carbides under these conditions. The concentration of carbon in the inner core has been evaluated using the equations of state of these carbides. Li et al. [18] studied the compressibility of cementite at pressures up to 30.5 GPa, and Scott et al. [19], using the experimental equation of state of cementite measured at pressures up to 73 GPa at 300 K, have concluded that carbon may well be a major light-alloying element in the core. Using *ab initio* simulations, Vočadlo et al. [20] found that the collapse of magnetism at ~ 60 GPa has a major effect on the equation of state of cementite. The magnetic collapse was experimentally established at about 45 GPa [21]; the observation of a large increase in incompressibility led to the conclusion that the presence of carbon will not improve the match with the observed seismic properties of the inner core. Based on their analysis of the thermal equation of state of Fe_3C and Fe, Huang et al. [15] concluded that carbon cannot be a major element in the core. The same conclusion was reached by Sata et al. [22], whereas Nakajima et al. [23], Fiquet et al. [24], and Gao et al. [25] have arrived at the opposite conclusion, namely that carbon can be a dominant light-alloying element in the inner core. Curiously, the above-mentioned discrepant conclusions were reached based on the equation of state of the same phase, cementite, which until recently was assumed to be stable at conditions of the inner core.

Yet, this assumption deserves to be challenged, as it is based essentially on nothing and turned out to be incorrect. Related to this issue, experiments [26] at 2200–3400 K and 25–70 GPa witnessed the stability of Fe_3C under those conditions. However, on the basis of their experimental phase diagrams, Lord et al. [27] demonstrated that cementite is most likely irrelevant for the inner core, and one should consider Fe_7C_3 instead. Nakajima et al. [28] studied this phase and its equation of state at pressures up to 71.5 GPa, while Mookherjee et al. [29] computed it up to the pressures of the inner core using *ab initio* simulations. Both studies concluded that the incorporation of carbon does provide a good match with the density of the inner core. Mookherjee et al. [29] estimated the amount of carbon needed for this match to be 1.5 wt.% (6.6 mol.%).

But what if at higher pressures, corresponding to the actual conditions of the inner core, yet another composition or structure is stable? Weerasinghe et al. [30] used the

random sampling approach [31] and came to the conclusion that Fe_2C is more stable than other compositions, but as they admitted that random sampling was not powerful enough to predict the structure of Fe_7C_3 , and a re-examination of the Fe–C system is warranted. We examine this question here and give new estimates of the maximum carbon content in the inner core.

Hydrogen is the element with the highest abundance in the Solar System ($10^4 \times \text{Si}$). Therefore, it seems logical to suppose that hydrogen could be the main element responsible for the density deficit observed in the Earth's core. Estimates by Stevenson [2] showed that the presence of FeH could explain the observable density of the inner core, but the low solubility of hydrogen in iron at atmospheric pressures makes this possibility less likely. Further studies pointed out that at high pressure the solubility of hydrogen in iron increases considerably [32], and the iron hydride phase FeH_x (with a stoichiometry approaching 1:1 ratio and a double hexagonal close-packed (dhcp) structure with interstitial hydrogen in octahedral sites) could be stable [33]. Depending on experimental conditions, different close-packed iron hydride phases were synthesized—dhcp, hcp, and face-centered cubic (fcc) [34–36], and at least up to 80 GPa the most stable phase has the dhcp structure [34, 37]. Skorodumova et al. [39] demonstrated by *ab initio* calculations that hydrogen stabilizes close-packed structures (hcp, dhcp, and fcc) of iron at high pressures and fills the octahedral voids in the structure. Isaev et al. [38] predicted that the fcc phase of FeH is stable above 83 GPa.

X-ray diffraction experiments performed in the diamond anvil cell at room temperature and pressures up to 80 GPa [37] showed two discontinuities (at 30 and 50 GPa) in the c/a axial ratio of FeH_x , and inferences were made to the lower hydrogen content (0.12–0.48 wt.%) than previously thought [33, 40]. Synchrotron Mössbauer measurements [41] demonstrated the loss of magnetism at 22 GPa, i.e., well below the *ab initio*-determined ferromagnetic–nonmagnetic transition at ~ 60 GPa [42].

Iron hydrides could be formed in the Earth's core by the reaction of iron with water during the early stages of Earth's accretion [33, 40, 43]: $(2+x)\text{Fe} + \text{H}_2\text{O} = 2\text{FeH} + \text{Fe}_x\text{O}$. Yagi and Hishinuma [44] studied the interaction between hydrogen and iron in the $\text{Fe}-\text{Mg}(\text{OH})_2-\text{SiO}_2$ system in the pressure range 2.2–4.9 GPa and temperatures up to 1350 °C, where the water was supplied by the decomposition of $\text{Mg}(\text{OH})_2$ brucite. They established that at 2.2 GPa and above 550 °C iron hydride (albeit with a chemical composition estimated to be $\text{FeH}_{0.3}-\text{FeH}_{0.4}$) was formed. Therefore, the formation of iron hydride at pressures as low as 2.2 GPa implies that if water was present in the proto-Earth together with silicates and iron, iron hydride would be formed at relatively shallow depths. Assuming a primordial Earth characterized by a hydrous magma ocean, Okuchi [45] calculated that, if the pressure at the bottom of the magma ocean was higher than 7.5 GPa, then more than 95 mol.% of the water could have reacted with iron to form FeH_x , which later sank to build the proto-core.

Therefore, it seems likely that currently there are no compelling geochemical reasons against the presence of significant amounts of either carbon or hydrogen in Earth's inner core.

Here, we consider this question from the point of view of mineral physics. It has been suggested [46] that hydrogen and carbon cannot be simultaneously present in the core. With

this in mind, we consider separately the Fe–C and Fe–H systems, finding the stable iron carbides and hydrides at pressures of the inner core. We consider crystal chemistry of stable iron carbides and hydrides and determine, on the basis of the most accurate available data, how much carbon or hydrogen is needed in order to match the observed density of the inner core of the Earth. Our calculations are based on the evolutionary crystal structure prediction method USPEX [47–50] and density functional theory [51, 52] within the generalized gradient approximation (GGA) [53]. The calculations successfully reproduce the known facts about these systems and predict hitherto unknown crucial pieces of information about the behavior of carbon and hydrogen in the Earth's inner core.

2. Methodology

As a simple test of the performance of the GGA, Fig. 1 compares theoretical (at $T=0$) and experimental (at $T=300$ K) equations of state of Fe_3C , Fe_7C_3 , and FeH . Computations performed here are done only for nonmagnetic states, because all experimental and theoretical evidences indicate collapse of magnetism in the Fe–C and Fe–H systems at several tens of gigapascals, i.e. well below the pressures of the inner core (330–364 GPa). From Fig. 1, one can see that agreement between theoretical and experimental equations of state is quite good, especially at pressures above ~ 100 GPa, and improves on increasing pressure.

Using the USPEX method [47–50] combined with GGA calculations, we found the lowest-enthalpy crystal structures at pressures of 300 GPa and 400 GPa, corresponding to compositions FeC , Fe_2C , Fe_3C , Fe_4C , FeC_2 , FeC_3 , FeC_4 , and Fe_7C_3 for the Fe–C system, and Fe_4H , Fe_3H , Fe_2H , FeH , FeH_2 , FeH_3 , and FeH_4 for the Fe–H system. Such calculations for pure Fe and C [47] and for H (Oganov, unpublished) have produced the known lowest-energy structures: hcp-Fe, diamond, and $Cmca$ -12-H (at 300 GPa) and $Cmca$ -H (at 400 GPa), respectively, in agreement with available experimental (e.g. for iron [17, 54, 55]) and theoretical [56] evidence. For each composition, at a given pressure, we identified the most favorable crystal structure and computed its enthalpy of formation from the elements. These enthalpies, normalized per atom, are given in Fig. 2, where stable compositions form a convex hull (i.e. a set of points lying below all lines joining any pair of other points in the diagram).

Structure prediction calculations were performed for Fe_4C (and Fe_4H) with 10 and 15 atoms per cell, Fe_3C (and Fe_3H) with 12 and 16 atoms per cell, Fe_7C_3 with 10 and 20 atoms per cell, Fe_2C (and Fe_2H) with 9 and 12 atoms per cell, FeC (and FeH) with 12 and 16 atoms per cell, FeC_2 (and FeH_2) with 9 and 12 atoms per cell, FeC_3 (and FeH_3) with 12 and 16 atoms per cell, and for FeC_4 (and FeH_4) with 10 and 15 atoms per cell. A typical USPEX simulation included 30–40 structures per generation, the lowest-enthalpy 60% of which were used for producing the next generation of

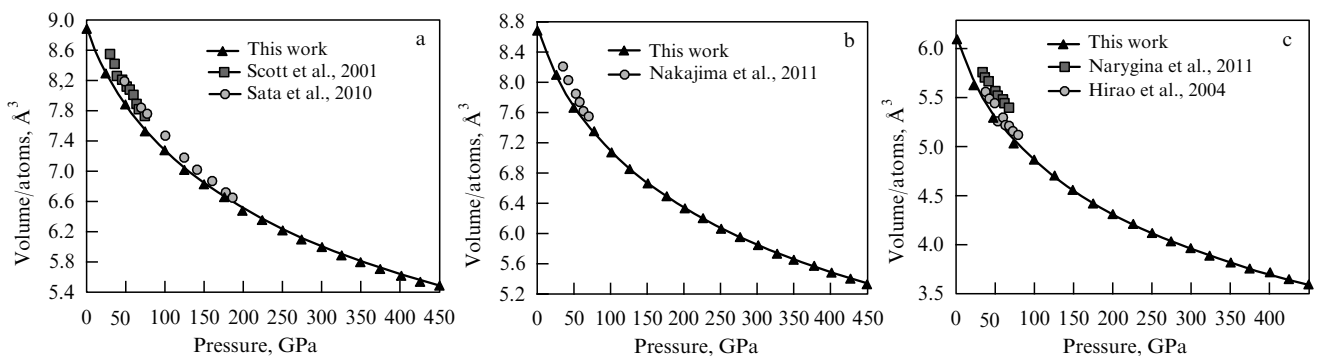


Figure 1. Comparison of the theoretical (at $T=0$) and experimental (at $T=300$ K) equations of state: (a) cementite Fe_3C , in comparison with high-pressure data of Scott et al. [19] and Sata et al. [22]; (b) $P6_3mc$ - Fe_7C_3 , in comparison with high-pressure data of Nakajima et al. [23], and (c) rocksalt type FeH , in comparison with high-pressure data of Narygina et al. [46] for the same phase, and Hirao et al. [37] for the related dhcp- FeH phase. Theoretical data are for the nonmagnetic state, which has been shown to be stable above 67 GPa for Fe_7C_3 [29] and above 60 GPa [20] or 25 GPa [21] for Fe_3C , and at 22 GPa [41] or 60 GPa [42] for FeH .

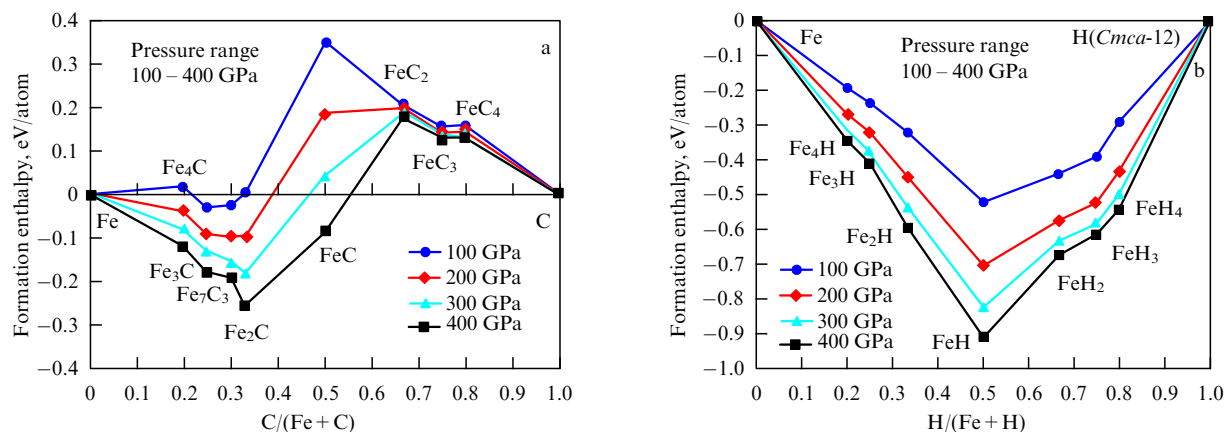


Figure 2. Predicted enthalpies of formation of (a) Fe–C, and (b) Fe–H compounds.

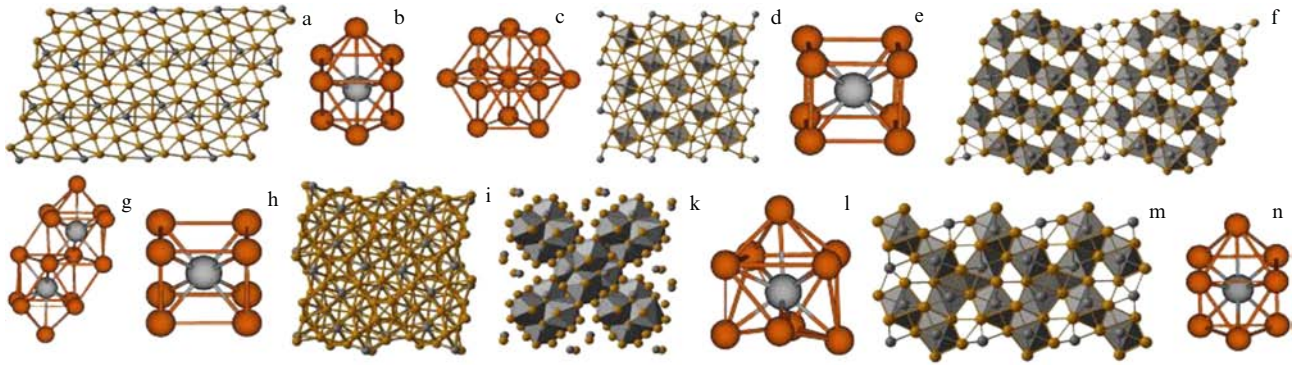


Figure 3. (See color version at www.ufn.ru.) New structures of iron carbides found in this work. Brown circles correspond to iron atoms, and dark grey circles to carbon atoms. (a) Fe_4C ($P2_1/m$) structure and (b) 8-coordinate environment of the carbon and (c) 12-coordinate (hexagonal cuboctahedral) environment of the iron atoms in it; (d) Fe_4C ($I4/m$) structure and (e) 8-coordinate environment of the carbon atom in it; (f) Fe_3C ($C2/m$) structure and (g, h) 9- and 8-coordinate environments of carbon atoms in it; (i, k) ball-and-stick and polyhedral representations of the Fe_3C ($I-4$) structure and (l) 9-coordinate environment of carbon atoms in it; (m) Fe_2C ($Pnma$) structure and (n) 8-coordinate environments of carbon atoms in it.

structures (70% of the offspring produced by heredity, 10% by atomic permutation, and 20% by lattice mutation). All structures produced by USPEX were then relaxed and their enthalpies computed using density functional theory within the generalized gradient approximation (GGA) [53] and employing the projector-augmented wave (PAW) method [57, 58], as implemented in the VASP code [59]. We used PAW potentials with an [Ar] core (radius 2.3 a.u.) and [He] core (radius 1.52 a.u.) for Fe and C atoms, respectively, and a PAW potential for H with the core radius of 1.1 a.u. Plane-wave kinetic energy cut-offs of 600 eV and 350 eV were used for Fe–C and Fe–H systems, respectively, and demonstrated to give excellent convergence of stress tensors and structural energy differences.

During structure relaxations done within USPEX simulations, we used homogeneous Monkhorst–Pack k-point meshes with reciprocal-space resolution of $2\pi \times 0.08 \text{ \AA}^{-1}$ and Methfessel–Paxton electronic smearing [60] with $\sigma = 0.1 \text{ eV}$. Having identified several lowest-enthalpy structures using USPEX, we recalculated their enthalpies in a range of pressures using a denser sampling of the Brillouin zone with the resolution of $2\pi \times 0.05 \text{ \AA}^{-1}$. In addition to structures found by USPEX, we also considered some experimentally known structures: $Pnmm$ for Fe_2C , cementite ($Pnma$) and bainite ($P6_322$) for Fe_3C (cementite was also seen in USPEX simulations), $P-43m$ for Fe_4C , and Cr_7C_3 type (of D101 type, space group $Pnma$), and $P6_3mc$ for Fe_7C_3 (which was also found by USPEX). In all cases, USPEX successfully produced structures that have the lowest enthalpy among all known or hypothetical structures. This gives us confidence in the reliability of the results discussed below.

3. Structures and compositions of stable iron carbides at ultrahigh pressures

For almost all Fe–C alloy compositions, at inner core pressures we found more stable structures than those known experimentally at lower pressures. The new structures are presented in Fig. 3. For Fe_3C , experiments [22] showed cementite to remain stable at least to 187 GPa (the highest pressure probed in the experiments [22]), which has led researchers to believe the cementite structure (space group $Pnma$; see Table 1) to be stable all the way up to the pressures of the inner core. Here, we established the upper limit of its stability as 310 GPa. Above 310 GPa (and this interval

Table 1. Structural parameters of some of the phases found by USPEX.

Phase (space group), pressure, unit cell parameters	Wyckoff position	x	y	z
Fe_2C ($Pnma$), 300 GPa, $a = 5.169 \text{ \AA}$, $b = 2.232 \text{ \AA}$, $c = 5.945 \text{ \AA}$	Fe 4c	0.834	0.25	0.951
	Fe 4c	0.499	0.75	0.839
	C 4c	0.796	0.75	0.176
Fe_7C_3 ($P6_3mc$), 300 GPa, $a = b = 5.987 \text{ \AA}$, $c = 3.773 \text{ \AA}$	Fe 2b	1/3	2/3	0.253
	Fe 6c	0.460	0.540	0.722
	Fe 6c	0.122	0.878	0.428
	C 6c	0.191	0.809	0.00
Fe_3C -cementite ($Pnma$), 300 GPa, $a = 4.325 \text{ \AA}$, $b = 5.778 \text{ \AA}$, $c = 3.843 \text{ \AA}$	Fe 4c	0.022	0.75	0.368
	Fe 8d	0.191	0.558	0.843
	C 4c	0.885	0.75	0.942
Fe_3C ($C2/m$), 400 GPa, $a = 7.321 \text{ \AA}$, $b = 2.155 \text{ \AA}$, $c = 11.720 \text{ \AA}$, $\beta = 104.76^\circ$	Fe 4i	0.485	0.00	0.778
	Fe 4i	0.731	0.00	0.722
	Fe 4i	0.644	0.00	0.529
	Fe 4i	0.495	0.50	0.626
	Fe 4i	0.380	0.50	0.899
	Fe 4i	0.131	0.50	0.953
	C 4i	0.682	0.50	0.839
Fe_3C ($I-4$), 400 GPa, $a = b = 7.104 \text{ \AA}$, $c = 3.555 \text{ \AA}$	Fe 8g	0.357	0.481	0.738
	Fe 8g	0.186	0.285	0.487
	Fe 8g	0.412	0.104	0.489
	C 8g	0.527	0.292	0.760
Fe_4C ($P2_1/m$), 400 GPa, $a = 5.293 \text{ \AA}$, $b = 2.196 \text{ \AA}$, $c = 5.423 \text{ \AA}$, $\beta = 103.01^\circ$	Fe 2e	0.876	0.75	0.844
	Fe 2e	0.184	0.75	0.511
	Fe 2e	0.671	0.25	0.074
	Fe 2e	0.522	0.25	0.678
	C 2e	0.102	0.25	0.743
Fe_4C ($I4/m$), 400 GPa, $a = b = 5.188 \text{ \AA}$, $c = 2.132 \text{ \AA}$	Fe 8h	0.423	0.722	0.00
	C 2a	0.00	0.00	0.00
FeH ($Fm-3m$), 300 GPa, $a = 3.162 \text{ \AA}$	Fe 4a	0.00	0.00	0.00
	H 4b	0.50	0.50	0.50
FeH_3 ($Pm-3m$), 300 GPa, $a = 2.215 \text{ \AA}$	Fe 1a	0.00	0.00	0.00
	H 3c	0.00	0.50	0.50
FeH_3 ($Pm-3n$), 400 GPa, $a = 2.702 \text{ \AA}$	Fe 2a	0.00	0.00	0.00
	H 6d	0.25	0.50	0.00
FeH_4 ($P2_1/m$), 300 GPa, $a = 3.479 \text{ \AA}$, $b = 3.062 \text{ \AA}$, $c = 2.331 \text{ \AA}$, $\beta = 101.63^\circ$	Fe 2e	0.252	0.25	0.551
	H 4f	0.370	0.958	0.118
	H 2e	0.198	0.75	0.561
	H 2a	0.00	0.00	0.00

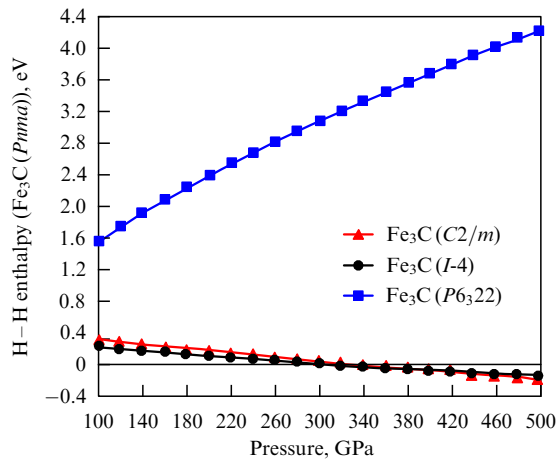


Figure 4. Enthalpies of Fe_3C polymorphs — $C2/m$, $I-4$, and $P6_322$ — as a function of pressure. Enthalpies are shown per formula unit and relative to cementite ($Pnma$).

includes the actual pressures in Earth's inner core, 330–364 GPa), USPEX found two more stable structures: with space groups $I-4$ (stable at 310–410 GPa) and $C2/m$ (stable above 410 GPa) (Fig. 4). One of the phases experimentally established at 1 atm, namely bainite (space group $P6_322$), is less stable than cementite, $I-4$ or $C2/m$ phases of Fe_3C at all pressures. The $Cmcm$ structure, predicted using random sampling as the most stable structure of Fe_3C above 326 GPa [30], turned out to be less stable than the structures predicted here at all pressures. At 300 GPa, it is 18 meV per formula unit (f.u.) less stable than cementite, and 7 meV/f.u. less than the $I-4$ structure. At 350 GPa, it is 16 meV/f.u. higher in enthalpy than the $I-4$ phase. At 400 GPa, it is 14 meV/f.u. less stable than the $C2/m$ structure, and 19 meV/f.u. less stable than the $I-4$ phase. This failure of the random sampling approach is well known and has been documented for several other systems, such as SiH_4 , SnH_4 , and N, for which evolutionary simulations using USPEX reported more stable structures [50]. Since the random sampling calculations of Weerasinghe et al. [30] for both Fe_7C_3 and Fe_3C failed to find stable structures, their other conclusions about Fe–C phases are in doubt, too.

For Fe_2C , the $Pnmm$ structure, experimentally verified at 1 atm, turned out to be much less stable at core pressures than the $Pnma$ structure predicted by USPEX (see Table 1) — by 0.59 eV/atom at 300 GPa, and 0.75 eV/atom at 400 GPa. For Fe_4C , the $P2_1/m$ and $I4/m$ structures (see Table 1) predicted by USPEX at 300 GPa and 400 GPa, respectively, are vastly (by 1.5–1.7 eV/atom) superior to the experimentally known $P-43m$ structure with 5 atoms in the unit cell. The stability of the $Pnma$ phase of Fe_2C is consistent with the results of Weerasinghe et al. [30].

Fe_7C_3 is unique among the compounds considered here in that the structure observed experimentally at 1 atm (space group $P6_3mc$; see Table 1) remains also stable at pressures of the Earth's inner core. This structure was successfully found in our USPEX simulations, in contrast to the previous random sampling calculations [30], and is more stable than the other phase of Fe_7C_3 experimentally found at 1 atm, with the $Pnma$ space group and 40 atoms per unit cell.

For the other compositions (FeC , FeC_2 , FeC_3 , FeC_4), we are not aware of any experimentally established phases. None of these compositions are found to be stable with respect to

decomposition into the elements or into a mixture of C and Fe_2C in the pressure range investigated. In some cases, e.g. FeC_4 , we observed phase separation in the predicted lowest-enthalpy structure into layers of iron and diamond within one simulation cell.

To summarize, applying USPEX algorithm we have found new lowest-enthalpy structures for FeC_4 ($P2_1/m$ and $I4/m$), Fe_3C ($I-4$ and $C2/m$), and Fe_2C ($Pnma$) at inner core pressures (see Fig. 3). These structures are extremely interesting and contain carbon atoms in 8- and 9-fold coordination. The Fe_4C ($P2_1/m$) structure shows Fe–C layering and can be described as hexagonal closest-packed arrangement of iron atoms strongly distorted by the insertion of carbon atoms, while Fe_4C ($I4/m$) structure can be obtained from a body-centered cubic (bcc) structure. Some compositional layering can also be seen in the Fe_3C ($C2/m$) structure, while the Fe_3C ($I-4$) structure contains remarkable tetragonal channels. The Fe_2C ($Pnma$) structure, which we have predicted to be the stable iron carbide at pressures of the inner core, displays no compositional layering and contains carbon atoms in the 8-fold coordination.

It is clear from our data that Fe_3C is not a stable carbide at pressures of the Earth's inner core — contrary to the common belief. Figure 2a shows the formation enthalpies of all studied Fe–C compounds. Using the convex hull construction, it is easy to see from this graph that among different iron carbides:

at 100 GPa, Fe_3C and Fe_7C_3 are stable

at 200 GPa, Fe_3C and Fe_2C are stable

at 300 GPa and 400 GPa, only Fe_2C is stable

These results clearly indicate that the traditional thinking, based on Fe_3C or Fe_7C_3 as the most stable iron carbide at pressures of the Earth's inner core, must be abandoned.

4. Structures and compositions of stable iron hydrides at ultrahigh pressures

In agreement with previous works (see, e.g., Ref. [33]), we found that FeH is stable at inner core pressures, but in addition to it phases with compositions FeH_3 and FeH_4 are also stable when hydrogen fugacity is high, and phases with compositions Fe_xH ($x > 1$), such as Fe_4H , are only marginally less stable than the isochemical mixture of Fe and FeH. Crystal chemistry for $\text{Fe}/\text{H} > 1$ and < 1 is very different, and below we consider both, although for the inner core only phases with $\text{Fe}/\text{H} > 1$ are relevant.

For Fe_xH with $x \geq 1$, the lowest-enthalpy structures have Fe atoms forming close-packed sublattices (fcc in FeH, and hcp in Fe_4H), with H atoms filling the octahedral voids. The stable structure of FeH at pressures of the inner core is of rocksalt type, with the fcc-packing of iron atoms, in agreement with previous calculations [38]. One could expect that hydrogen will stabilize close-packed structures of iron in the Earth's core.

The predicted metastable structures allow us to draw some conclusions on the energetics of H–H interactions and the effects of partial hydrogen incorporation into the structure of iron. For illustration, let us consider Fe_4H , the lowest-enthalpy structure of which possesses space group $P-3m1$ and can be described as an hcp-packing of iron atoms, with H atoms filling every fourth octahedral layer (Fig. 5a). There are very many alternative and slightly less stable ways of occupying one quarter of the octahedral voids in close-packed structures, and Fig. 5 illustrates some of them. For this composition, the most stable structures are based on the

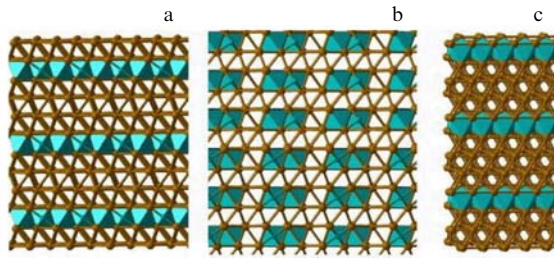


Figure 5. (See color version at www.ufn.ru.) Structures of Fe_4H : (a) lowest-enthalpy $P\bar{3}m1$ structure, and (b, c) higher-enthalpy structures based on different arrangements of the H atoms in the hcp structure. Turquoise octahedra highlight positions of the H atoms, whereas iron atoms are shown by the orange spheres.

hcp-packing of Fe atoms (enthalpies of other packings are higher by > 20 meV/atom). Within the hcp-packing of Fe atoms, H atoms show the tendency to segregate into layers, which implies that incorporation of moderate amounts of hydrogen into iron sublattice will increase the anisotropy of the hcp structure. Face sharing of the H-centered octahedra tends to be avoided: structures with the maximum extent of face sharing (Fig. 5c) are destabilized by ~ 20 meV/atom, whereas structures fully avoiding face sharings (such as the one shown in Fig. 5b) have enthalpies within 8 meV/atom of the ground state.

For Fe_xH with $x < 1$, FeH_3 and FeH_4 are thermodynamically stable at the pressures of the inner core, are of substantial chemical interest, and their structures are built on very different principles. The stable phase of FeH_3 at 300 GPa belongs to the Cu_3Au structure type (space group $Pm\bar{3}m$; see Fig. 6b), while the structure preferred at 400 GPa is like that of Cr_3Si (also known as A15 type, space group $Pm\bar{3}n$; see Fig. 6c). The Cu_3Au type structure is an fcc superstructure, with all atoms in the 12-fold coordination, suggesting that iron and hydrogen atoms in this FeH_3 structure have comparable sizes (unlike in FeH and Fe_xH compounds with $x > 1$, where hydrogen was small enough to fit the octahedral voids of the close-packed iron sublattice). In the Cr_3Si type structure, known for many superconductors (such as Nb_3Sn and Nb_3Ge , which held record-high superconducting T_c values before the advent of cuprate superconductors), coordination numbers are more ambiguous, but are at any rate similar for Fe and H atoms. In this case, the most interesting feature is the presence of FeH_{12} icosahedral units. The closest H–H distance at 400 GPa equals 1.35 Å.

Stability of FeH_4 above ~ 180 GPa is certainly surprising and raises the question of whether Fe in this compound is in the unusual tetravalent state. The stable FeH_4 structure found by USPEX calculations at 300 GPa and 400 GPa (Fig. 6d) is complex, has low symmetry (space group $P2_1/m$), and belongs to a new structure type. It contains many H–H

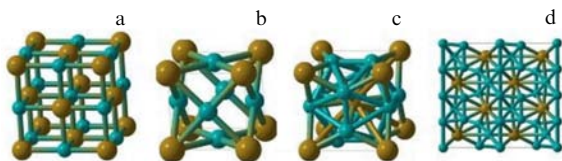


Figure 6. Structures of stable high-pressure iron hydrides: (a) rocksalt-type FeH , (b) $Pm\bar{3}m$ and (c) $Pm\bar{3}n$ phases of FeH_3 , and (d) the $P2_1/m$ phase of FeH_4 .

bonds, the shortest of which (at $p = 400$ GPa) are 1.16 Å long.

To resolve the valence state of Fe atoms in FeH_4 and to get deeper insight into chemical bonding in the metallic phases of FeH_3 and FeH_4 described above, we used Brown's bond valence method [61], the main formula of which is

$$n = \exp\left(\frac{R_0 - R}{b}\right), \quad (1)$$

where n is the bond valence, R is the bond length, b is a constant (usually taken as $b = 0.37$ Å), and R_0 is a bond-specific constant (which, however, depends on pressure). The sum of bond valences then defines the valence of the atom. To apply formula (1), we first calibrate R_0 values on a structure where the valences are known, namely FeH . We obtained $R_0 = 1.32$ (1.27) Å for Fe–Fe, 0.92 (0.89) Å for Fe–H, and 0.51 (0.50) Å for H–H bonds at 300 GPa (400 GPa). The values for Fe–Fe and Fe–H bonds were obtained directly, while the one for H–H is deduced from them and is therefore less accurate.

Applying equation (1) to FeH_3 , we obtained the sum of bond valences in Fe equal to 2.6 at $p = 300$ GPa and 2.7 at $p = 400$ GPa—in reasonable agreement with the expected valence of 3. Turning to FeH_4 , we again obtain the sum of bond valences equal to 2.7 at $p = 400$ GPa, i.e. again trivalent iron, a prediction that can be verified experimentally using Mössbauer spectroscopy. Bond valence calculations also explain how FeH_4 can have trivalent (rather than tetravalent) iron—extensive H–H bonding satisfies part of the valence needs of hydrogen atoms and decreases the need for additional electrons from Fe atoms. Very crudely, half of hydrogen's valence is satisfied by H–H bonds, and to satisfy the valence of four hydrogen atoms only 2 (instead of 4) electrons from Fe are needed. Each Fe atom gives up two valence electrons for Fe–H bonding, and 1 additional electron is used for Fe–Fe bonding, thus making the total valence of Fe atoms equal to 3.

Stable hydrides that contain more H atoms than prescribed by naive application of chemical valence have been predicted, e.g. for an Li–H system at high pressures [62], and include such exotic compounds as LiH_2 , LiH_6 , and LiH_8 . Just as in FeH_4 , those compounds also contain H–H bonds. Even in hydrides of 'normal' stoichiometries, such as GeH_4 [63] and SnH_4 [64], high pressure promotes the formation of H–H bonds that should be accompanied by a decrease in the metal valence (we showed that in the high-pressure $Cmcm$ phase of SnH_4 , tin is counterintuitively divalent, rather than tetravalent [50]).

5. How much carbon and hydrogen are needed to explain the density of the inner core?

If C and H are to be considered as potential major light elements in the core, several conditions have to be met: (i) the amount of light elements needed to explain the observed core density at the expected core temperatures (5000–6000 K [65]) should not be unacceptably large (roughly, < 20 mol.%); (ii) this amount should not display large and nonmonotonic variations with depth, and (iii) the resulting mean atomic mass \bar{M} should be reasonably close to the one determined from Birch's law, i.e. 49 [5]. As we shall demonstrate below, carbon satisfies all these necessary conditions, which means that it is a good candidate to be a major alloying element in

Table 2. Theoretical third-order Birch–Murnaghan equations of state of the nonmagnetic high-pressure phases in the Fe–C and Fe–H systems. Theoretical data refer to 0 K isotherms without zero-point corrections. For diamond, experimental data [67] are shown in parentheses. For comparison of theoretical and experimental equations of state, see also Fig. 1.

Phase	$V_0, \text{\AA}^3/\text{atom}$	K_0, GPa	K'_0
hcp-Fe	10.15	305.7	4.3
Fe ₃ C-cementite	8.88	326.1	4.31
C2/m-Fe ₃ C	8.97	283.2	4.56
I4-Fe ₃ C	8.78	333.6	4.34
Fe ₇ C ₃	8.68	317.6	4.37
Fe ₂ C	8.44	333.9	4.23
Diamond	5.71 (5.68)	431.8 (446)	3.62 (3)
fcc-FeH	6.11	270.8	4.25

the inner core. Hydrogen marginally satisfies conditions (i) and (ii), but not (iii).

Our procedure is as follows. Since theoretical absolute densities suffer from small but non-negligible systematic errors of theory, and accurate experiment-based P - V - T equation of state is known for pure hcp-iron [66], we based our estimates on the known density of pure iron at relevant pressures and temperatures, and treated the compositional effect on the density as linear, and determined it from the theoretical density differences between hcp-Fe and stable iron carbide (Fe₂C) or hydride (FeH) at relevant pressures and $T = 0$ K. Parameters of the relevant theoretical equations of state are given in Table 2, and are close to the previous theoretical values [20, 29, 70].

We determine the molar concentration of the light element needed to explain the density of the Earth's inner core by matching the observed density of the inner core to the density of the mixture of hcp-Fe and the stable carbide/hydride at relevant pressures and temperatures. This corresponds to the concentration needed if carbon or hydrogen were the only light-alloying element and, since several alloying elements are likely to be present, gives the upper bound for the concentration of each element. For instance, considering the Fe–Fe₂C mixture for the case of carbon, we could determine the molar concentration of carbon that matches the two densities:

$$\rho_{\text{IC}} = \rho_{\text{Fe}}^T + \frac{\partial \rho}{\partial x} x \Rightarrow \rho_{\text{IC}} - \rho_{\text{Fe}}^T = \frac{\rho_{\text{Fe}_2\text{C}}^0 - \rho_{\text{Fe}}^0}{0.33} x, \quad (2)$$

where ρ_{IC} is the density of the inner core at each depth from the preliminary reference Earth model (PREM) [68], ρ_{Fe}^T is the density of pure iron at the temperature T [66], and ρ_{Fe}^0 and $\rho_{\text{Fe}_2\text{C}}^0$ are the computed zero-Kelvin densities of Fe and Fe₂C. The number 0.33 appearing in Eqn (2) indicates the molar fraction of carbon in Fe₂C. The essence of equation (2) is to compute the P - V - T -equation of state of a Fe–C(H) alloy from the well-constrained P - V - T -equation of state of pure iron [66], supplementing it with the theoretically computed (at $T = 0$) compositional derivatives of the density. This is a trick to solve a well-recognized problem: density-functional calculations give birth to systematic errors equivalent to the shift of the absolute equation of state by several GPa [69], which makes direct comparison of theoretical equations of state with seismic data dangerous. However, volume (or density) differences (caused by the effects of the composition or temperature on the density) are usually very accurate due to compensation of errors, and thus equation (2) gives reliable estimates.

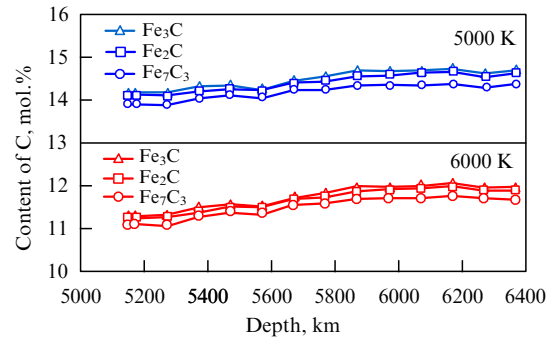


Figure 7. Matching molar concentration of carbon as a function of depth in the inner core. Results based on Fe₃C, Fe₇C₃, and Fe₂C carbon-bearing phases are traced along the 5000 K and 6000 K isotherms.

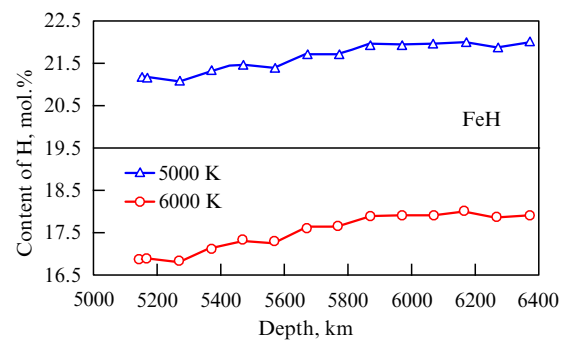


Figure 8. Matching molar concentration of hydrogen as a function of depth in the inner core. Results are traced along the 5000 K and 6000 K isotherms.

The resulting carbon concentrations (estimated along the 5000 K and 6000 K isotherms) are very reasonable: 11–15 mol.% C (2.6–3.7 wt.% C), and do not show in addition large variations throughout the inner core. This result matches the carbon concentration in CI carbonaceous chondrites. Furthermore, the resulting \bar{M} is in the range 49.3–51.0, which is very close to the desired value of 49 [5]. All this indicates that a significant amount of carbon can exist in the Earth's inner core. Note that these estimates for carbon are not very sensitive to the choice of the reference carbide: Fig. 7 shows that if we take Fe₃C or Fe₇C₃ instead of Fe₂C, essentially the same results will be obtained. Our estimates are compatible with the latest estimates based on the equation of state of Fe₇C₃: 3.2 wt.% [28], 1.5 wt.% [29], and 3.7 wt.% (Prakapenka, pers. commun.).

Similarly made estimates for the hydrogen-matching concentrations are given in Fig. 8. The matching concentrations vary between 17 and 22 mol.% (0.4–0.5 wt.%) if we use the equation of state for FeH (or 24–32 mol.% if we use Fe₄H). This is much higher than the recent estimate of 0.08–0.16 wt.% by Narygina et al. [46], but is compatible with the 0.12–0.48 wt.% proposed by Hirao et al. [37]. Yet, hydrogen content of 17–22 mol.% appears too large to be realistic, especially in view of the resulting average atomic mass \bar{M} in the range 43.8–46.5, which is too low compared to $\bar{M} = 49$ inferred from the Birch's law. We cannot rule out the presence of considerable amounts of hydrogen in the inner core, but it certainly cannot be the dominant light element.

At first sight, it might appear surprising that hydrogen, being much lighter than carbon, is required in greater

concentrations than carbon to reproduce the observed density deficit. This becomes elucidated if one considers the crystal chemistry of iron carbides and hydrides at ultrahigh pressures. Carbon atoms are much larger and significantly affect the crystal structure of the alloy, where they occupy rather large sites with 8- or 9-fold coordination. All this has significant effects on the density, because the insertion of carbon destroys the closest packing of the Fe atoms and significantly increases the unit cell volume. On the other hand, much smaller hydrogen atoms sit comfortably in the octahedral voids of the closest packing of iron atoms (in our structure searches, we also saw metastable phases hosting hydrogen in even smaller voids). Incorporation of hydrogen does not destroy the close packing of the Fe atoms and has only a minor effect on the unit cell volume. Its effect on the density is about two times smaller than that of carbon incorporation.

6. Conclusions

The question of the chemical composition of Earth's inner core has occupied the minds of scientists for decades, and in recent years there has been a resurgence of interest in carbon and hydrogen as potential light alloying elements in the iron-dominated core. The results obtained by different researchers differ greatly because of the assumptions and approximations made. Using state-of-the-art *ab initio* simulation techniques, including evolutionary crystal structure predictions and density functional theory, new insight has been gained into Fe–C and Fe–H systems at pressures of the Earth's inner core.

The evolutionary crystal structure prediction method USPEX was shown to be more reliable than the random sampling approach in searching for ground-state structures. New hitherto unsuspected ground states have been found using USPEX in both systems. Chemically (though not mineralogically) important and surprising tendency is the destabilization of FeH₂ and stabilization of FeH₄ under pressure; the stability of even higher iron hydrides has not been investigated here and certainly deserves a separate study. Crystal structures of iron carbides and hydrides at inner core pressures show a striking difference: while hydrogen atoms sit in the interstices of close-packed iron structures and have a minor effect on the density, carbon atoms occupy much larger sites in complex non-close-packed structures and, as a consequence, carbon has a much stronger effect on the density.

Therefore, to match the observed density of the inner core, one needs an unrealistically high concentration of hydrogen. At the same time, carbon (at least from the point of view of density of the inner core) cannot be ruled out as the dominant light element in the inner core (with the concentration in the range of 11–15 mol.%). Coupled with geochemical and meteoritic evidence, the presence of significant amounts of carbon in Earth's core seems plausible, logical, and perhaps even unavoidable. Then, if carbon and hydrogen cannot simultaneously be present in Earth's core, as recently claimed [46], the presence of hydrogen could be ruled out with great probability. But before that, the conclusions of paper [46] need to be reassessed. Further constraints can be provided by the density and compressional wave velocity in the liquid outer core, seismic wave velocities in the inner core, and chemical equilibria at the inner–outer core boundary [71]. Systematic analysis of the effect and possible presence of

other elements (S, Si, O), based on crystal structure predictions, is urgently needed. The results on the Fe–Si system have already been published [72], and studies into the Fe–O and Fe–S systems are underway.

Acknowledgments

This work was supported by the U.S. National Science Foundation (grant EAR-1114313) and DARPA (grant N66001-10-1-4037). Calculations were performed at Moscow State University (MSU Skif supercomputer), at the Joint Supercomputer Center of the Russian Academy of Sciences, and on the CFN cluster (Brookhaven National Laboratory), which is supported by the U.S. Department of Energy, Office of Basic Energy Sciences, under contract No. DE-AC02-98CH10086.

References

1. Birch F *J. Geophys. Res.* **69** 4377 (1964)
2. Stevenson D J *Science* **214** 611 (1981)
3. Jeanloz R *Annu. Rev. Earth Planet. Sci.* **18** 357 (1990)
4. Birch F *J. Geophys. Res.* **57** 227 (1952)
5. Poirier J-P *Introduction to the Physics of the Earth's Interior* 2nd ed. (Cambridge: Cambridge Univ. Press, 2000)
6. Buchwald V F *Handbook of Iron Meteorites: Their History, Distribution, Composition, and Structure* Vol. 1 (Berkeley, Calif.: Univ. of California Press, 1975)
7. Jephcoat A, Olson P *Nature* **325** 332 (1987)
8. Poirier J-P *Phys. Earth Planet. Inter.* **85** 319 (1994)
9. Wood B J *Earth Planet. Sci. Lett.* **117** 593 (1993)
10. Tingle T N *Chem. Geol.* **147** 3 (1998)
11. Hirayama Y, Fujii T, Kurita K *Geophys. Res. Lett.* **20** 2095 (1993)
12. McDonough W F, in *Treatise on Geochemistry* Vol. 2 (Ed. R W Carlson) (Amsterdam: Elsevier, 2003) p. 547
13. Hillgren V J, Gessmann C K, Li J, in *Origin of the Earth and Moon* (Eds R M Canup, K Righter) (Tucson: Univ. of Arizona Press, 2000) p. 245
14. Anisichkin V F *Combust. Explosion Shock Waves* **36** 516 (2000)
15. Huang L et al. *Geophys. Res. Lett.* **32** L21314 (2005)
16. Oganov A R et al. *Earth Planet. Sci. Lett.* **273** 38 (2008)
17. Tateno S et al. *Science* **330** 359 (2010)
18. Li J et al. *Phys. Chem. Minerals* **29** 166 (2002)
19. Scott H, Williams Q, Knittle E *Geophys. Res. Lett.* **28** 1875 (2001)
20. Vočadlo L et al. *Earth Planet. Sci. Lett.* **203** 567 (2002)
21. Lin J-F et al. *Phys. Rev. B* **70** 212405 (2004)
22. Sata N et al. *J. Geophys. Res.* **115** B09204 (2010)
23. Nakajima Y et al. *Phys. Earth Planet. Inter.* **174** 202 (2009)
24. Fiquet G et al. *Phys. Earth Planet. Inter.* **172** 125 (2009)
25. Gao L et al. *Geophys. Res. Lett.* **35** L17306 (2008)
26. Rouquette J et al. *Appl. Phys. Lett.* **92** 121912 (2008)
27. Lord O T et al. *Earth Planet. Sci. Lett.* **284** 157 (2009)
28. Nakajima Y et al. *Am. Mineral.* **96** 1158 (2011)
29. Mookherjee M et al. *J. Geophys. Res.* **116** B04201 (2011)
30. Weerasinghe G L, Needs R J, Pickard C J *Phys. Rev. B* **84** 174110 (2011)
31. Freeman C M et al. *J. Mater. Chem.* **3** 531 (1993)
32. Fukai Y et al. *Jpn. J. Appl. Phys.* **21** L318 (1982)
33. Badding J V, Mao H K, Hemley R J, in *High-Pressure Research: Application to Earth and Planetary Sciences* (Geophysical Monograph Ser., Vol. 67, Eds Y Syono, M H Manghnani) (Washington, DC: Terra Sci. Publ. Co./American Geophysical Union, 1992) p. 363
34. Badding J V, Hemley R J, Mao H K *Science* **253** 421 (1991)
35. Yamakata M et al. *Proc. Jpn. Acad. B* **68** 172 (1992)
36. Fukai Y, Yamakata M, Yagi T *Z. Phys. Chem. N.F.* **179** 119 (1993)
37. Hirao N et al. *Geophys. Res. Lett.* **31** L06616 (2004)
38. Isaev E I et al. *Proc. Natl. Acad. Sci. USA* **104** 9168 (2007)
39. Skorodumova N V, Ahuja R, Johansson B *Geophys. Res. Lett.* **31** L08601 (2004)
40. Fukai Y *Nature* **308** 174 (1984)
41. Mao W L et al. *Geophys. Res. Lett.* **31** L15618 (2004)
42. Elsässer C et al. *J. Phys. Condens. Matter* **10** 5113 (1998)

43. Stevenson D J *Nature* **268** 130 (1977)
44. Yagi T, Hishinuma T *Geophys. Res. Lett.* **22** 1933 (1995)
45. Okuchi T *Science* **278** 1781 (1997)
46. Narygina O et al. *Earth Planet. Sci. Lett.* **307** 409 (2011)
47. Oganov A R, Glass C W J. *Chem. Phys.* **124** 244704 (2006)
48. Glass C W, Oganov A R, Hansen N *Comput. Phys. Commun.* **175** 713 (2006)
49. Lyakhov A O, Oganov A R, Valle M *Comput. Phys. Commun.* **181** 1623 (2010)
50. Oganov A R, Lyakhov A O, Valle M *Acc. Chem. Res.* **44** 227 (2011)
51. Hohenberg P, Kohn W *Phys. Rev.* **136** B864 (1964)
52. Kohn W, Sham L J *Phys. Rev.* **140** A1133 (1965)
53. Perdew J P, Burke K, Ernzerhof M *Phys. Rev. Lett.* **77** 3865 (1996)
54. Hemley R J, Mao H K *Int. Geol. Rev.* **43** 1 (2001)
55. Ma Y et al. *Phys. Earth Planet. Inter.* **143–144** 455 (2004)
56. Pickard C J, Needs R J *Nature Phys.* **3** 473 (2007)
57. Blöchl P E *Phys. Rev. B* **50** 17953 (1994)
58. Kresse G, Joubert D *Phys. Rev. B* **59** 1758 (1999)
59. Kresse G, Furthmüller J *Phys. Rev. B* **54** 11169 (1996)
60. Methfessel M, Paxton A T *Phys. Rev. B* **40** 3616 (1989)
61. Brown I D *Acta Cryst. B* **48** 553 (1992)
62. Zurek E et al. *Proc. Natl. Acad. Sci.* **106** 17640 (2009)
63. Gao G et al. *Phys. Rev. Lett.* **101** 107002 (2008)
64. Gao G et al. *Proc. Natl. Acad. Sci.* **107** 1317 (2010)
65. Alfè D et al. *Philos. Trans. R. Soc. Lond. A* **360** 1227 (2002)
66. Dewaele A et al. *Phys. Rev. Lett.* **97** 215504 (2006)
67. Occelli F, Loubeyre P, LeToullec R *Nature Mater.* **2** 151 (2003)
68. Dziewonski A M, Anderson D L *Phys. Earth Planet. Inter.* **25** 297 (1981)
69. Oganov A R, Brodholt J P, Price G D *Earth Planet. Sci. Lett.* **184** 555 (2001)
70. Alfè D, Kresse G, Gillan M J *Phys. Rev. B* **61** 132 (2000)
71. Alfè D, Gillan M J, Price G D *Earth Planet. Sci. Lett.* **195** 91 (2002)
72. Zhang F, Oganov A R *Geophys. Res. Lett.* **37** L02305 (2010)